Naval Research Laboratory
Washington, DC 20375-5320

NRL/6120/MR—2021/3

Real Time Control of NMR Relaxation for Improved Sensitivity and Resolution

JOEL B. MILLER

CHRISTOPHER A. KLUG

JAMES P. YESINOWSKI (RETIRED NRL EMPLOYEE)

Materials Chemistry Branch
Chemistry Division

July 6, 2021

REPORT DOCUMENTATION PAGE

Form Approved
OMB No. 0704-0188

1. REPORT DATE *(DD-MM-YYYY)*	**2. REPORT TYPE**	**3. DATES COVERED** *(From - To)*
06-07-2021	NRL Memorandum Report	10/01/2014 – 06/16/2021

4. TITLE AND SUBTITLE

Real Time Control of NMR Relaxation for Improved Sensitivity and Resolution

5a. CONTRACT NUMBER

5b. GRANT NUMBER

5c. PROGRAM ELEMENT NUMBER

6. AUTHOR(S)

Joel B. Miller, Christopher A. Klug, and James P. Yesinowski*

5d. PROJECT NUMBER

5e. TASK NUMBER

5f. WORK UNIT NUMBER
1P88

7. PERFORMING ORGANIZATION NAME(S) AND ADDRESS(ES)

Naval Research Laboratory
4555 Overlook Avenue, SW
Washington, DC 20375-5320

8. PERFORMING ORGANIZATION REPORT NUMBER

NRL/6120/MR--2021/3

9. SPONSORING / MONITORING AGENCY NAME(S) AND ADDRESS(ES)

Naval Research Laboratory
4555 Overlook Avenue, SW
Washington, DC 20375-5320

10. SPONSOR / MONITOR'S ACRONYM(S)
NRL

11. SPONSOR / MONITOR'S REPORT NUMBER(S)

12. DISTRIBUTION / AVAILABILITY STATEMENT

DISTRIBUTION STATEMENT A: Approved for public release; distribution is unlimited.

13. SUPPLEMENTARY NOTES
*Retired NRL Employee

14. ABSTRACT

Molecules / molecular structures were investigated for enhancing NMR relaxation in the presence of light while not adversely affecting NMR spectral properties in the absence of light, with the ultimate goal of enhancing the sensitivity of NMR spectroscopy. The molecules / molecular structures are: [Fe(salicylaldehyde)2(triethylenetetramine)]PF6, [Fe(1-propyltetrazole)6](BF4)2, [Fe(4-amino-1,2,4-triazole)3](BF4)2, Platinum meso-tetraaryl porphyrin – rhodamine B piperazine dyad, Pentacene-spiro-pentacene and tetracene-anthracene-tetracene, and 1-(dibenzo[b,d] furan-2-yl)phenylmethanone. This report contains new chemical and physical characterization of these materials.

15. SUBJECT TERMS

Magnetic resonance Relaxation
Photoexcited electrons

16. SECURITY CLASSIFICATION OF:			**17. LIMITATION OF ABSTRACT**	**18. NUMBER OF PAGES**	**19a. NAME OF RESPONSIBLE PERSON**
					Joel B. Miller
a. REPORT	**b. ABSTRACT**	**c. THIS PAGE**	U	25	**19b. TELEPHONE NUMBER** *(include area code)*
U	U	U			(202) 767-2337

Standard Form 298 (Rev. 8-98)
Prescribed by ANSI Std. Z39.18

This page intentionally left blank.

Table of Contents

List of Figures

Introduction

With the rapid development in methods to prepare new nanomaterials comes the requirement for precise atomic-level characterization of the structures of these materials. Nuclear Magnetic Resonance (NMR) spectroscopy has the potential to yield this information, provided its inherent sensitivity limitations can be overcome.

A variety of cutting edge methods are known for enhancing NMR sensitivity. While offering significant gains in sensitivity, they each have their particular drawbacks: hyperpolarized noble gases[1] have restrictions on the types of applicable systems; paramagnetic relaxation agents [2,3,4,5] exhibit decreased spectral resolution; some techniques have requirements for specialized equipment (*e.g.* gyrotrons for Dynamic Nuclear Polarization (DNP)[6]), special experimental conditions (*e.g.* the Haupt effect[7] and chemically induced dynamic nuclear polarization (CIDNP)[8]), or specialized materials (*e.g.* parahydrogen[9], transferred polarization from optically-pumped semiconductors[10]). Recently the NV center in powdered diamonds is also receiving considerable attention as a possible means of improving NMR sensitivity at room temperature, based on the potential for transferring hyperpolarization from ^{13}C nuclear spins to nuclear spins of interest.[11]

One of the most widely applicable techniques for increasing NMR detection sensitivity is the use of paramagnetic ions. Enhancing NMR sensitivity through reduction of the nuclear spin-lattice relaxation time, T_1, using paramagnetic ions has a long history. Its continued relevance to NMR spectroscopy was highlighted recently[2]. The sensitivity gain is limited by the maximum concentration of paramagnetic ions that results in an acceptable level of line broadening from the magnetic hyperfine fields of the ion. In this report we demonstrate the potential for improved NMR sensitivity by the control of the spin-lattice relaxation time, T_1, at low temperatures for enhanced nuclear polarization, via the reversible creation of photoexcited relaxation agents using non-coherent optical excitation. Such materials open up the possibility that paramagnetic molecules acting beneficially as relaxation agents during the relaxation delay become favorably diamagnetic during signal acquisition. The concentration of these materials will not be limited by their paramagnetic line broadening effects, and hence they could be used in much higher concentrations than other permanently paramagnetic species.

There are potential advantages of photoexcited relaxation agents beyond sensitivity enhancement. The relaxation times of those nuclei closest to the photoexcited relaxation agents are reduced the most. Therefore, this method can be surface selective, and could preferentially enhance signals from nuclei in the outer shells of the nanoparticles shown in Figure 1(a). Another significant experimental option for spatial selectivity is to target the location of the relaxing agents to a specific region of the material of interest using a photoexcitable molecule that specifically and preferentially interacts with that region (through hydrophobic, hydrophilic, ionic, covalent, etc., interactions)—see Figure 1(b).

We identified two main groups of molecules that have the potential to act as photoexcited relaxation agents: organic molecules with long-lived photoexcited triplet states, and transition

Manuscript approved June 22, 2021.

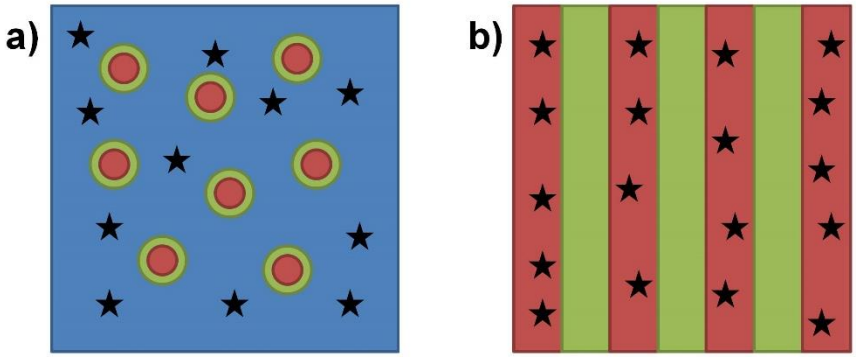

Figure 1: a) Schematic of 3D matrix consisting of the sample of interest, in this case core/shell nanomaterials, photoexcited molecules (stars) and a matrix (in blue); b) Schematic of two-component system where photoexcited molecules are selectively incorporated into one component. The key to real-time control is that the photoexcited molecules act as local paramagnetic relaxation agents for the sample only during the controllable illumination period and for a very short period thereafter during which the excited state decays to the diamagnetic ground state. The sample is at some low temperature to achieve a large Boltzmann population difference vis-à-vis room temperature. The light is turned off for the short time each NMR scan is acquired, thus avoiding the spectral broadening effects of paramagnetic agents and allowing high resolution NMR spectra (with appropriate samples and NMR techniques) to be obtained.

metal complexes that exhibit the light-induced excited spin state trapping (LIESST)[12] effect. In the following section we outline the requirements for these molecules to be successful photoexcited relaxation agents. In subsequent sections we describe work on a number of potential photoexcited relaxation agents that we identified. In the final section we discuss the specific data analysis techniques used to analyze photoexcited relaxation data.

Photoexcited relaxation agents

There are several requirements for a successful photoexcited relaxation agent related to the nature of its excited state, the spin physics of the photoexcited electrons, and the physical and chemical nature of the relaxation agent. The first and foremost requirement is the existence of an accessible and chemically stable photoexcited state with unpaired electron spins. A vast number of molecules meet this requirement. Second, we must be able to establish a large population of photoexcited electrons. This, in turn, requires very efficient photoexcitation and a long lifetime in the excited state.

Establishing a large steady state population of agents in the photoexcited state does not guarantee that the agents efficiently induce nuclear spin relaxation. The first requirement given above for photoexcited relaxation agents provides for unpaired electrons; a new and third requirement is that those unpaired electron spins must be in a spin state having a net magnetic moment and must have magnetic moments that fluctuate at a rate comparable to the

nuclear Larmor frequency in order to efficiently induce nuclear spin relaxation. For even numbers of unpaired electrons, such as the two spins that form the triplet state (S = 1), there will be a spin sublevel of the excited state that has a net electron magnetic moment of zero (S_z = 0). The rules of photoexcitation may initially populate such a state, but that is not a concern as long as the electron spin lattice relaxation time is shorter than the lifetime in the excited state, providing a mechanism to populate the other spin sublevels. Likewise, fluctuation of the electron magnetic moments occurs because of rapid spin lattice or spin-spin relaxation.

To be useful in real NMR studies, the fourth requirement is that the efficient nuclear spin relaxation capability of a photoexcited relaxation agent must be coupled to the nuclei in the material of interest. Therefore, the relaxation agent must be in near atomic contact with the material to be relaxed. The relaxation agent must be able to adsorb on the surface of the material, be miscible in the material, or be miscible with the material and a solvent in a frozen solution. This places constraints on the chemical structure of the relaxation agent. Furthermore, the relaxation agent must maintain its excited state properties while on the surface or in solution, placing additional constraints on its physical and chemical structure. In the following sections we discuss some of the more important materials we investigated as possible photoexcited relaxation agents.

[Fe(salicylaldehyde)$_2$(triethylenetetramine)]PF$_6$

The first spin crossover complex (SCO) compound chosen was [Fe(salicylaldehyde)$_2$(triethylenetetramine)]PF$_6$ (abbreviated [Fe(sal$_2$trien)]PF$_6$), which is a SCO Fe(III) complex exhibiting a temperature-dependent magnetic susceptibility due to the equilibrium between the low spin (^{2}T) and high spin (^{6}A) form.[13] This system is not a true photoexcited relaxation agent: the transition between high spin and low spin states is thermally activated, and the low spin state is not a zero spin state. We anticipated, based on literature observations, that high-spin Fe(III) at lower temperatures would have a higher relaxivity than the corresponding Fe(II) complex. We obtained results on SCO of Fe(III) using an ultrabright white light emitting diode light source with a liquid filled light guide cable and an optical system to deliver a collimated light beam through the transparent sapphire window of the Janis cryogenic NMR probe to the sample in a quartz cuvette. The optical absorption characteristics and proton T_1 measurements were carried out as a function of temperature in the 7.4 T magnetic field of the NMR spectrometer (300 MHz proton Larmor frequency). We synthesized the ligands and the complex, and then observed the SCO effect vs. temperature by monitoring the absorption spectrum in acetone (Figure 2a), whose broad peak shifted from ca. 490 nm at 320 K (high-spin form) to ca. 610 nm at 200 K. However, the proton T_1 relaxation times of the acetone only varied over this entire range from 1.1 s to 1.5 s. The reasons for this insensitivity despite the large change in magnetic susceptibility may have to do with the greater relaxivity of the ^{2}T state suggested by the proton NMR broadening of the peaks from the complex itself. Since spin lifetimes of the two states have been measured in a different solvent

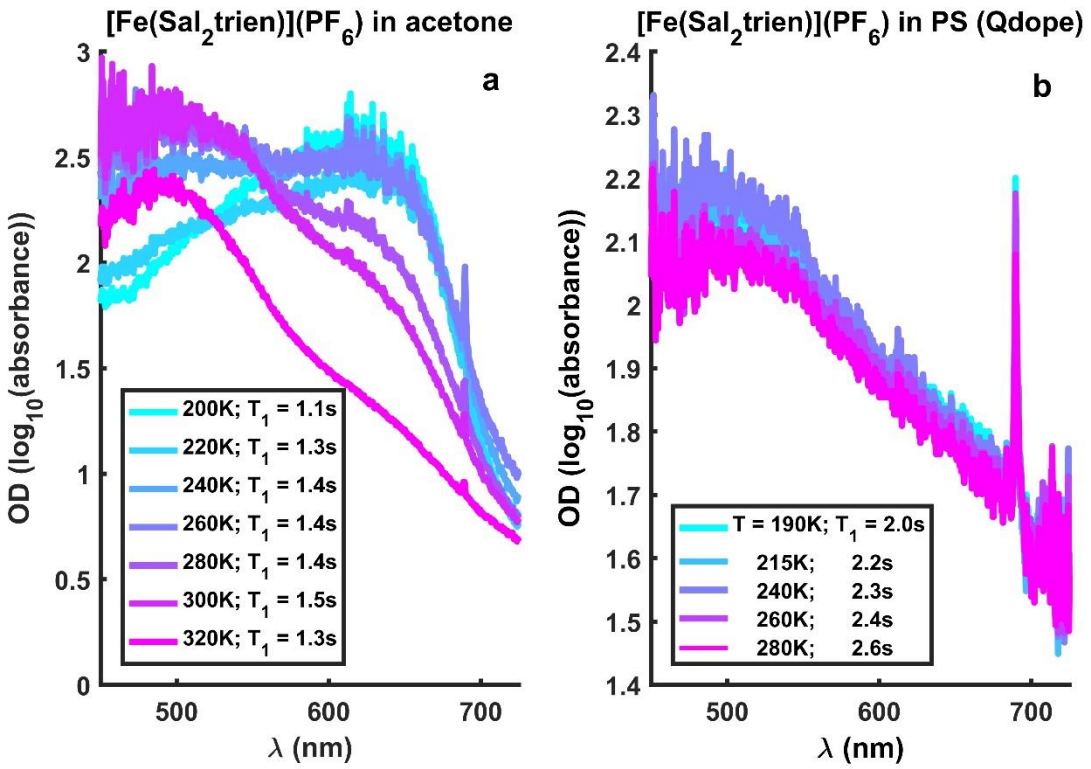

Figure 2: a) optical absorption of [Fe(salicylaldehyde)$_2$(triethylenetetramine)]PF_6 dissolved in liquid acetone as a function of temperature showing the transition from low-spin to high-spin state; b)) optical absorption of a solid solution of [Fe(salicylaldehyde)$_2$(triethylenetetramine)]PF_6 dissolved in polystyrene as a function of temperature showing no spin state transition.

and are in a range where significant NMR relaxivity would result, we investigated this SCO complex in a glassy matrix of polystyrene. However, unlike the acetone solution, the optical absorption did not change from 190 K to 280 K (Figure 2b); a broad peak at ca. 490 nm from the high spin form was seen, and the proton T_1 varied only from 2.0 to 2.6 s.

[Fe(1-propyltetrazole)$_6$](BF$_4$)$_2$

We studied two Fe(II) spin-crossover (SCO) complexes that exhibits a LIESST effect. The first complex, [Fe(1-propyltetrazole)$_6$](BF$_4$)$_2$, reversibly switches at low temperature between an *S*=0 (low-spin) state and an *S*=2 (high-spin) state upon illumination, and has received attention as a light-actuated single-molecule magnet.[14] We successfully demonstrated our photoexcited relaxation agent concept, which involved preparation of this Fe(II) complex in a proton-rich surrounding matrix, whose proton NMR spin-lattice relaxation time T_1 is reduced by the photomagnetism of the photoexcited relaxation agent. It is clear from the optical evidence that the thermally induced transformation from high-spin to low-spin upon cooling is not blocked by the surrounding matrix, as occurred in the Fe(III) SCO complex initially studied. Furthermore, the transformation induced by visible light is also not blocked.

Most of the results of these studies have been published[15] and will not be described in detail here. However, new ways of analyzing the complex multiexponential data used for these studies will be described in more detail in the Data Analysis section, below. The main published result was that a weak enhanced nuclear relaxation in polystyrene was observed with this photoexcited relaxation agent. The observed effect was weak because the presence of [Fe(1-propyltetrazole)$_6$](BF$_4$)$_2$ in polystyrene significantly enhanced relaxation even in the low-spin state. The enhanced relaxation can be explained by the presence of methyl groups in [Fe(1-propyltetrazole)$_6$](BF$_4$)$_2$, whose rapid rotation is well-known to provide an efficient dipolar relaxation mechanism for protons in solids at low temperatures. This led us to investigate subsequently [Fe(4-amino-1,2,4-triazole)$_3$](BF$_4$)$_2$, a LIESST compound without methyl groups.

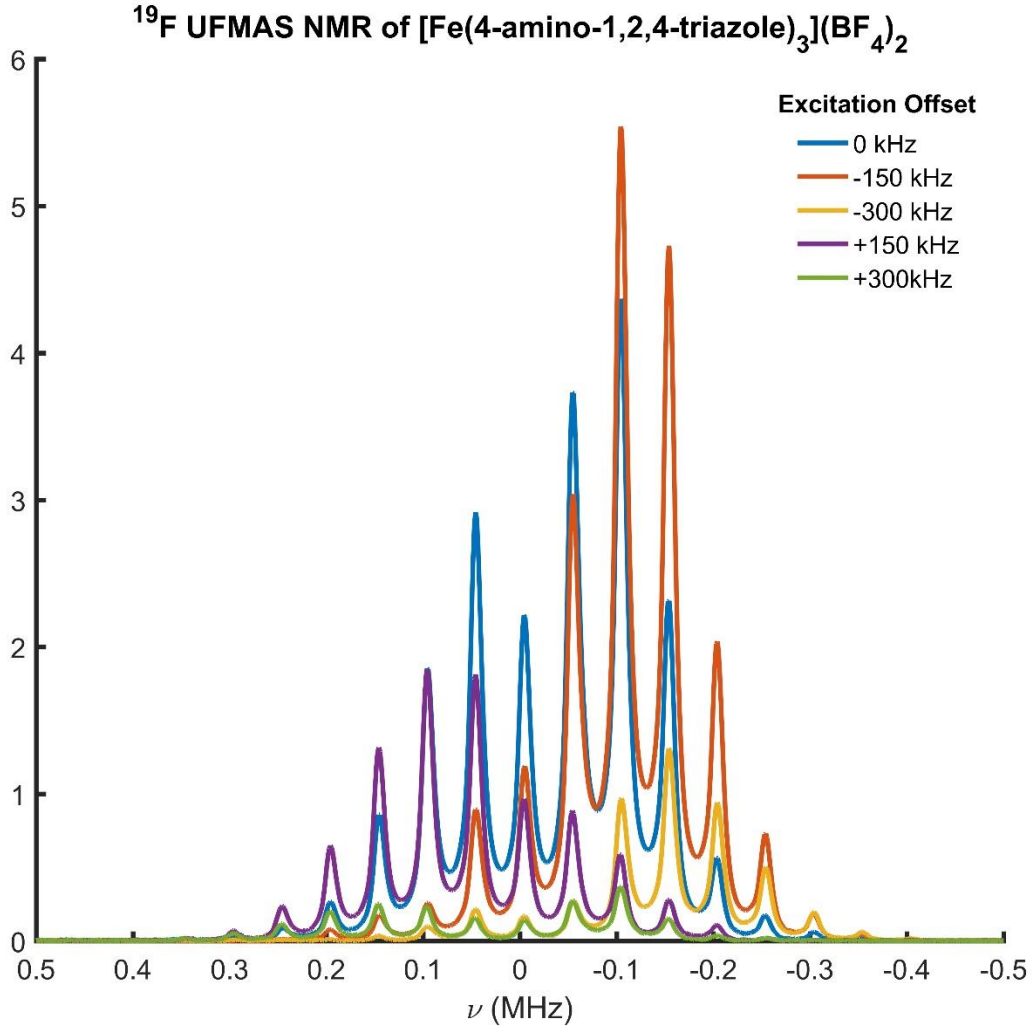

Figure 3: The ^{19}F UF-MAS spectrum of [Fe(4-amino-1,2,4-triazole)$_3$](BF4)$_2$ obtained as a series of spectra with stepped-frequency offsets showing a very broad resonance at room temperature, plus the associated spinning sidebands at multiples of the spinning frequency.

$[Fe(4\text{-amino-}1,2,4\text{-triazole})_3](BF_4)_2$

The second LIESST compound we studied was $[Fe(4\text{-amino-}1,2,4\text{-triazole})_3](BF_4)_2$.[16] Like the other LIESST compound we studied, the second also reversibly switches at low temperature between an S=0 (low-spin) state and an S=2 (high-spin) state upon illumination. This compound was chosen to overcome several limitations encountered with $[Fe(1\text{-propyltetrazole})_6](BF_4)_2$. The first problem is that the low transition temperature limits the types of NMR experiments available to study the transition. The second LIESST compound has a transition temperature around 250 K. The second problem is that the methyl groups on the first LIESST compound shorten the T_1 relaxation time, even in the low spin state. This partially conceals the photoexcited relaxation agent effect. The second LIESST compound contains no methyl groups.

We focused on obtaining ^1H and ^{19}F ultrafast magic-angle spinning (UF-MAS) NMR spectra of $[Fe(4\text{-amino-}1,2,4\text{-triazole})_3](BF_4)_2$ as a function of temperature. The line shapes of the pure LIESST compound reflect the spin state of the compound, allowing us to track the spin transition without the long experiment times needed to measure T_1. The ^{19}F UF-MAS spectrum (Figure 3, obtained as a series of spectra with stepped-frequency offsets) shows a very broad resonance at room temperature, plus the associated spinning sidebands at multiples of the spinning frequency, the latter of which extend over a significantly narrower frequency range below the transition temperature of 250 K (reference 12). Likewise, the ^1H stepped-frequency static (Figure 4) and UF-MAS (Figure 5) NMR spectra extend over a much wider frequency range at room temperature than when below the transition temperature. Plotting the second moment for the ^{19}F line shape as a function of temperature, taking into account the direction of the temperature change (warming or cooling) shows the expected hysteresis in the transition temperature (Figure 6).

The NMR results clearly show that a spin phase transition occurs at the reported temperature. However, at low temperature the ^1H and ^{19}F resonances are much broader than expected for an *S*=0 spin system. Furthermore, no significant change in ^1H T_1 was observed when crossing the transition. We considered two possible explanations: 1) only a fraction of the LIESST compound was undergoing the spin phase transition; 2) the material was contaminated with some Fe^{+3}. To test the second possibility, a second sample was synthesized under exclusion of oxygen in air that might have oxidized Fe(II) to Fe(III). However, this sample did not exhibit the anticipated longer T_1 for a diamagnetic sample at lower temperature. The two samples did show differences in both XPS and EPR experiments that suggest a greater presence of Fe(III) in the first sample. The XPS results for this sample yielded an atomic composition for Fe of 4.22% and for B of 10.36%, representing a ratio of 0.41 vs. the theoretical ratio of 0.5 for the Fe(II) complex. A lower ratio would be expected for a sample having an Fe(III) complex with a BF_4^- monoanion. The second sample had Fe 5.23% and B 9.94%, or a ratio of 0.53, closer to the value expected for all Fe(II) complex. The EPR spectrum at 9.510 GHz and 6 K of the first sample also showed complex peaks characteristic of both high-spin and low-spin Fe(III),

consistent with the XPS results (It should be noted that the EPR technique is much more sensitive to the presence of small amounts of Fe(III).) Repeated NMR experiments with thermal cycling of the second sample yielded irreproducible behavior, whether due to thermal hysteresis effects in the transition or perhaps other structural changes. Unfortunately understanding this behavior could not be pursued further beyond the conclusion of the program.

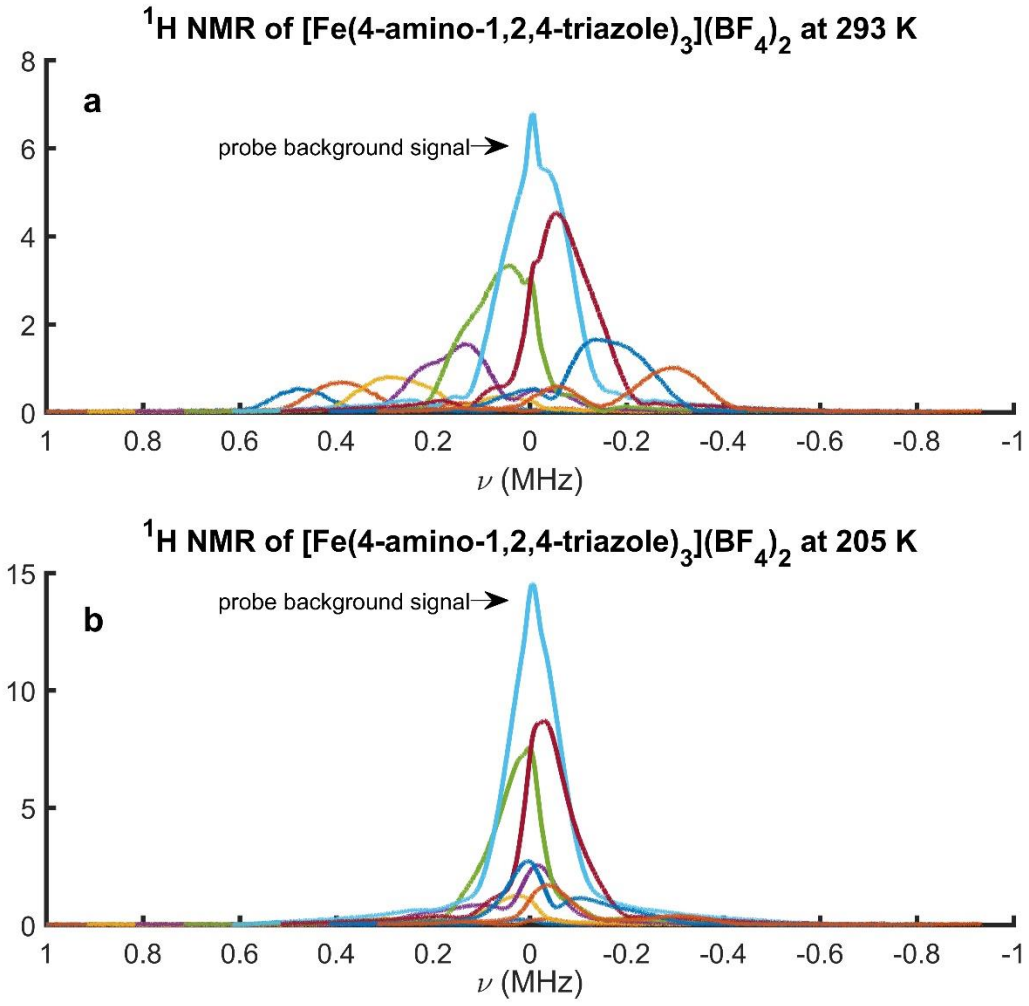

Figure 4: ^{1}H stepped-frequency static NMR spectra of [Fe(4-amino-1,2,4-triazole)$_3$](BF4)$_2$ extend over a much wider frequency range at room temperature (top) than when below the transition temperature (bottom).

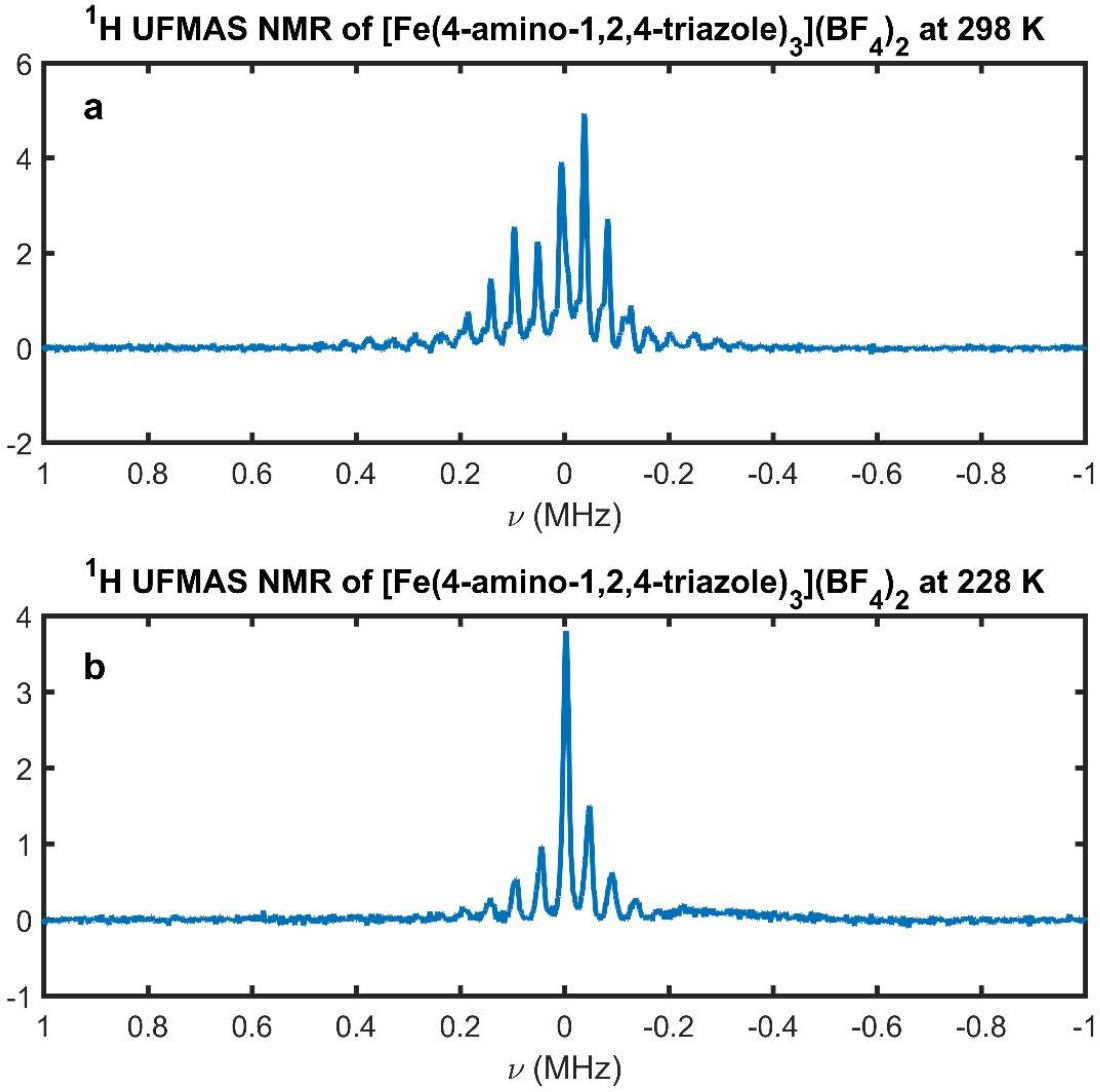

Figure 5: ^{1}H UF-MAS NMR spectra of [Fe(4-amino-1,2,4-triazole)$_3$](BF4)$_2$ show spinning sidebands over a much wider frequency range at room temperature (top) than when below the transition temperature (bottom).

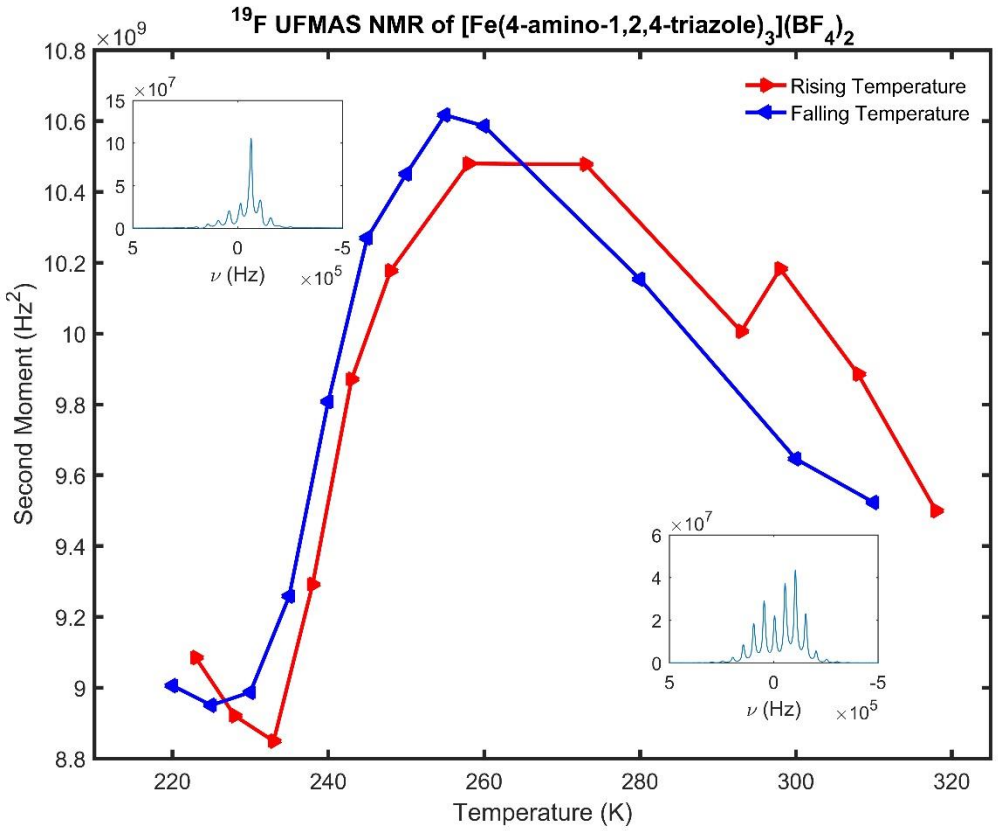

Figure 6: Second moment of the ^{19}F line shape of [Fe(4-amino-1,2,4-triazole)$_3$](BF4)$_2$ as a function of temperature, taking into account the direction of the temperature change (warming or cooling) shows the expected hysteresis in the transition temperature. The insets show the UF-MAS line shapes at the high and low temperature limits.

Platinum meso-tetraaryl porphyrin – rhodamine B piperazine dyad

Another material that we investigated was a platinum porphyrin – rhodamine B dyad.[17] The dyad consists of a platinum *meso*-tetraaryl porphyrin covalently linked to a rhodamine B piperazine derivative through an oligo-*p*-phenylene bridge. The material was of interest because of its structural and electronic similarity to bacterial photosynthetic reaction centers that have shown the CIDNP effect.[18] The idea is to create phosphorescent triplet states by photoinduced electron transfer (ET). By Forster energy transfer between the antenna dye portion and the porphyrin portion the emissive lifetimes of the triplet exciton state can be lengthened. These features are what is desirable for functioning as a photoexcited relaxation agent. One potential concern is the effects of magnetic field on the triplet formation and lifetime in these systems.[19]

Strictly speaking, the CIDNP effect does not fit the role of a photoexcited relaxation agent; the main effect of CIDNP is to relax the nuclear spins to a high, non-equilibrium polarization, but it

does not necessarily shorten their relaxation times. However, the advantages are the same: higher signal-to-noise ratio (SNR) per unit time without broadening from paramagnetic centers.

The multi-step synthesis was a very difficult one, but the two components were successfully covalently linked in the final step of the reaction. Samples of the complex were prepared as both solvent-dissolved and as films cast from polystyrene solutions containing the complex. At 80 K, where the solvent was frozen and the polystyrene very rigid, no significant shortening of the proton spin-lattice relaxation time T_1 was observed upon irradiation with visible light. One possibility is that the dyad complex is itself unstable in the solutions used to prepare the samples, dissociating into its components. Since the optical spectra of the individual components are virtually identical to that of the dyad complex, the optical spectra we obtained (not shown) were incapable of ruling out this possibility.

Pentacene-spiro-pentacene and tetracene-anthracene-tetracene

Following up on a presentation by Professor Campos from Columbia University describing his group's efforts to develop molecules for use in solar cells with unusually long excited state lifetimes,[20] we decided to obtain some of his materials for evaluation. The motivation was that the unusual triplet-state lifetimes of these molecules might shift their electron spectral density into a region close the inverse Larmor frequency of the protons and thereby increase the overall efficiency for cross-relaxation. Furthermore, the Campos group had already done significant work on measuring the electronic properties of these materials in the solid state and in blends with polymers.

We were provided with two materials: pentacene-spiro-pentacene[21] (PSP) and tetracene-anthracene-tetracene[22] (TAT). Both materials were described as light sensitive, TAT being the more sensitive of the two. TAT was also described as oxygen sensitive. NMR measurements were made on both materials at 80 K and 293 K under flowing nitrogen in our cryostat. No effects on the NMR relaxation were seen with either material. However, it was clear from the color of the material that the white light source we used in the NMR optical relaxation measurements had caused the TAT to decompose. It was unclear whether there was similar decomposition with PSP, or if the shorter triplet lifetime in that material resulted in a negligible NMR relaxation effect.

1-(dibenzo[b,d]furan-2-yl)phenylmethanone

Late in the program we came across a recent and highly-cited paper describing a number of small organic molecules with long-lived triplet states, one of the top priorities for photoexcited relaxation agents.[23] One molecule in particular, 1-(dibenzo[b,d]furan-2-yl)phenylmethanone (BDBF), drew our attention because the triplet lifetime is greater than 100 ms, even in frozen

solution, and the quantum efficiency is very high, suggesting the possibility of easily creating a high concentration of photoexcited relaxation agents.

The BDBF synthesized at NRL showed strong yellow-green phosphorescence when irradiated with UV light around 380 nm on the bench top that persisted for several seconds after the light was turned off. The phosphorescence was also observed at liquid nitrogen temperature for a sample of BDBF dissolved in glassy polystyrene (PS). Optical experiments within our combined NMR / optical probe confirmed phosphorescence with the sample in a magnetic field of 7 T (figure 7), but we were unable to quantify the phosphorescence due to the geometry of our probe. Our UV/Vis spectrometer is not capable of time-resolved measurements; therefore, we were not able to quantify the lifetime of the phosphorescence.

NMR measurements as a function of UV light irradiation at room temperature and liquid nitrogen temperature on BDBF in PS showed no change in the line shape or T_1 at either temperature. Although a lack of change in T_1 might be explained by a mismatch between the ^1H Larmor frequency and the electron correlation time, the lack of any change in the line shape is remarkable. The long lifetimes and high quantum efficiencies would lead one to anticipate a high population of photoexcited states in the NMR samples, which, if paramagnetic, would lead to significant broadening of the NMR peaks. We theorize that intersystem crossing from the excited singlet state to the triplet state populates only the non-magnetic $m_z = 0$ sublevel of the triplet state because transitions to the $m_z = +1, -1$ triplet sublevels are spin-forbidden. This implies that there is no net electron magnetization.[24] Normally, we would expect the electron spin lattice relaxation to thermally equilibrate the magnetic sublevels on a timescale shorter than the lifetime of the triplet state. Instead, our results suggest that the electron spin lattice relaxation time is long compared to the lifetime of the triplet state, much longer than a typical electron spin lattice relaxation time. If this is the case, BDBF might exhibit shorter electron T_1 values at lower field strengths, and thus have more favorable photoexcited relaxation agent properties at lower magnetic fields than we can access. It could also be a good candidate for optically-excited triplet state DNP.[17] Unfortunately, we do not have the hardware to test this hypothesis.

Experimental

The experimental procedure involved dissolving the complex and polystyrene in chloroform and rapidly removing the solvent by placing the solution on a hot plate, leading to a colored solid film which was then placed into our custom designed and homebuilt optical excitation/optical spectroscopy proton NMR probe. The spin-lattice relaxation behavior was observed using a saturation-recovery pulse sequence, and multiple data sets were collected at specific temperatures from 290 K to 30 K, in the dark or under illumination with visible light.

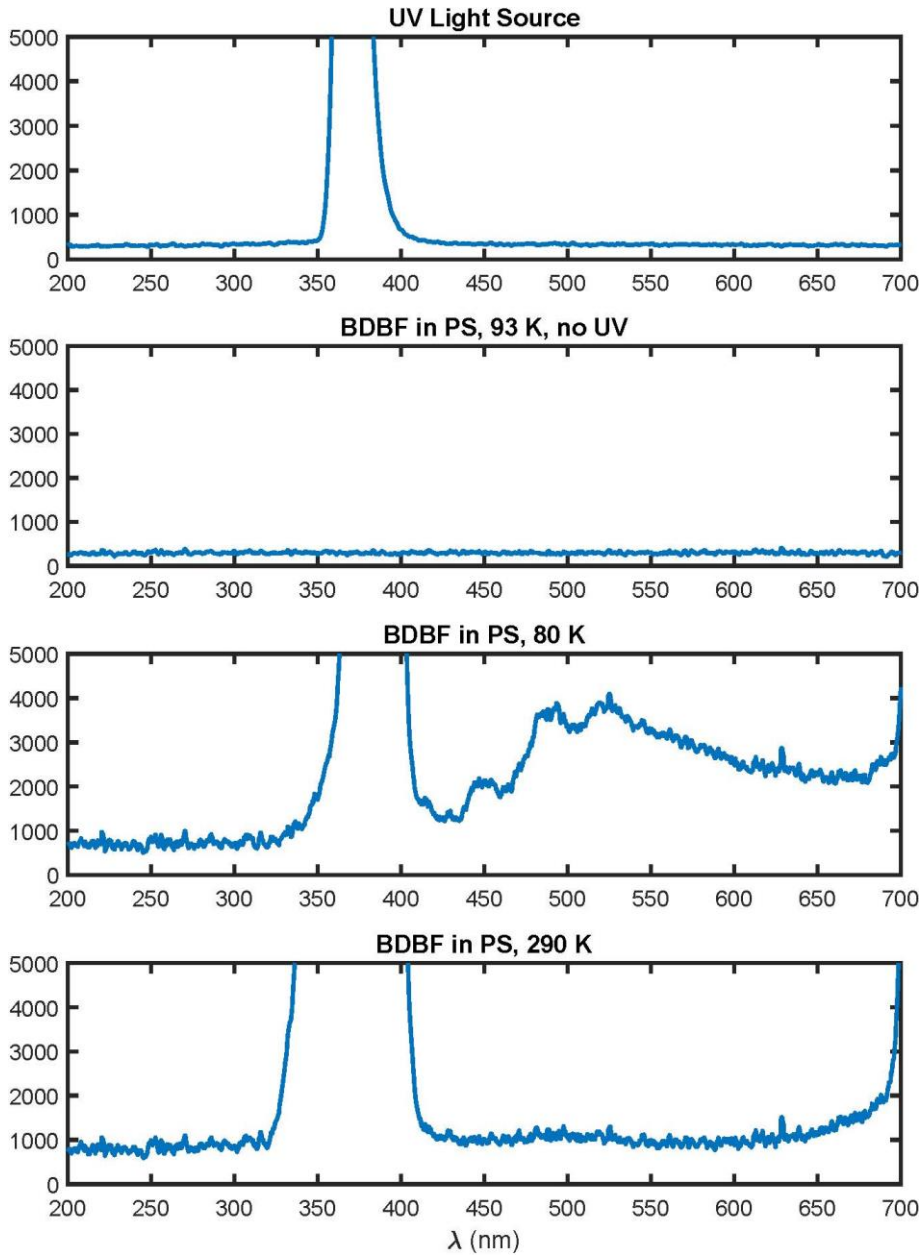

Figure 7: Optical experiments within our combined NMR / optical probe confirmed phosphorescence with the sample in a magnetic field of 7 T at liquid nitrogen temperature: a) emission spectrum of UV light source; b) emmission spectrum at 93 K of BDBF dissolved in glassy poltstyrene with no UV excitation showing no phosphorescence; c) emission spectrum at 80 K of BDBF dissolved in glassy polystyrene with UV excitation showing phosphorescence in the range of 450 to 600 nm; d) emission spectrum at 290 K of BDBF dissolved in glassy polystyrene with UV excitation showing no phosphorescence.

Data analysis

Typically, NMR relaxation data were processed in the time domain. It was often observed that a weak CW signal contaminated the NMR relaxation data; therefore, the last 50% of the data were fitted to a sinusoid. The sinusoid was extrapolated to the entire NMR relaxation data and

subtracted from it. The first point of the Free Induction Decay (FID) was affected by switching transients and was not used. The magnitude of the next 16 points of the FID were summed and used as a measure of the signal amplitude. We also measured the noise level for each FID. The FID decays into the noise within approximately the first 20% of the recorded data. The standard deviation of the last 50% of the recorded data, multiplied by the square root of 16 (to account for summing 16 points of data), was taken as a representation of the noise level for subsequent data analysis.

From the beginning, the program was plagued by lack of reproducibility of the relaxation measurements. Multiple measurements of the relaxation time were made for a given set of conditions to try to find a consistent value. We observed that, in addition to the aforementioned CW signal pickup, drifts in temperature and probe tuning sometimes occurred during long data acquisitions. Some problems with the data appeared to be caused by abrupt changes in the spectrometer transmitter and / or receiver characteristics. We have not been able to track down the source of these problems.

Much effort was applied to finding unbiased tests to determine a data set's suitability for use. We settled on two tests that were applied to groups of raw data. The first test measured the initial phase of the FID. The phase is sensitive to changes in the NMR probe properties, mostly induced by changes in temperature. For a set of NMR relaxation data the phases of the FID's were measured and any data whose phase differed by more than ±0.2 rad from the median value for the entire set was flagged. The second test measured the median absolute deviation of the FID amplitude.[25] Deviations in amplitude arise from changes in transmitter and receiver characteristics, as well as temperature effects on the NMR probe properties and the nuclear spin polarization. Any data set with a median absolute deviation greater than three was flagged.

To analyze our relaxation data we used Linear Programming (LP).[26] This type of analysis differs from the more traditional least squares (LS) fitting routines in that a finite number of possible solutions are given to the LP algorithm along with the data and a measure of the noise in the data. (In our case, possible solutions are single exponential signal recovery functions, each with a different time constant.) The LP algorithm attempts to apply weights to the provided solutions such that the weighted sum of all the provided solutions fits the data to within the noise level. If multiple solutions exist to the LP problem, the solution that minimizes the weights multiplied by a cost function (normally taken as one) is reported.

We chose LP to analyze our photoexcited relaxation agent data for two reasons. First, we do not have a good model for our relaxation data. Proton relaxation in most molecules exhibits a single relaxation time due to spin diffusion. In our materials multiple relaxation times are possible if: 1) the photoexcited relaxation agent is not uniformly distributed in the matrix or is in too low a concentration for spin diffusion to equilibrate different nanoscopic regions of the sample; 2) illumination of the matrix is not uniform; 3) there is a temperature gradient across the sample; 4) the photoexcited relaxation agent interferes with spin diffusion. With LS one

must specify in advance how many relaxation times are needed to fit the data, but LP adjusts the weights to accommodate multiple relaxation times. Second, LS will always provide a "best fit" to the data regardless of whether the model that is fit to the data is correct, whereas LP will report no feasible solution if the data cannot be fitted to within the provided noise level.

The chances of the noise contribution to the data being less than our measured one standard deviation noise level are small, so the noise level was scaled for the LP algorithm. An iterative method was used to determine the minimum scaling factor that produced a fit, if the data could be fit, and that scaling factor was later analyzed to determine if the data were usable. Along with the requirements of phase and amplitude median absolute deviation, we found that requiring the scaling factor to be less than 12 provided consistent data sets.

To compare the results of LP analysis from multiple data sets we chose to characterize those results through the first and second moments of the LP weights. If the ratio of the square root of the second moment to the first moment is much smaller than 1, the relaxation is well characterized by a single relaxation time; otherwise, the relaxation has multiple relaxation times or possibly a distribution or relaxation times.

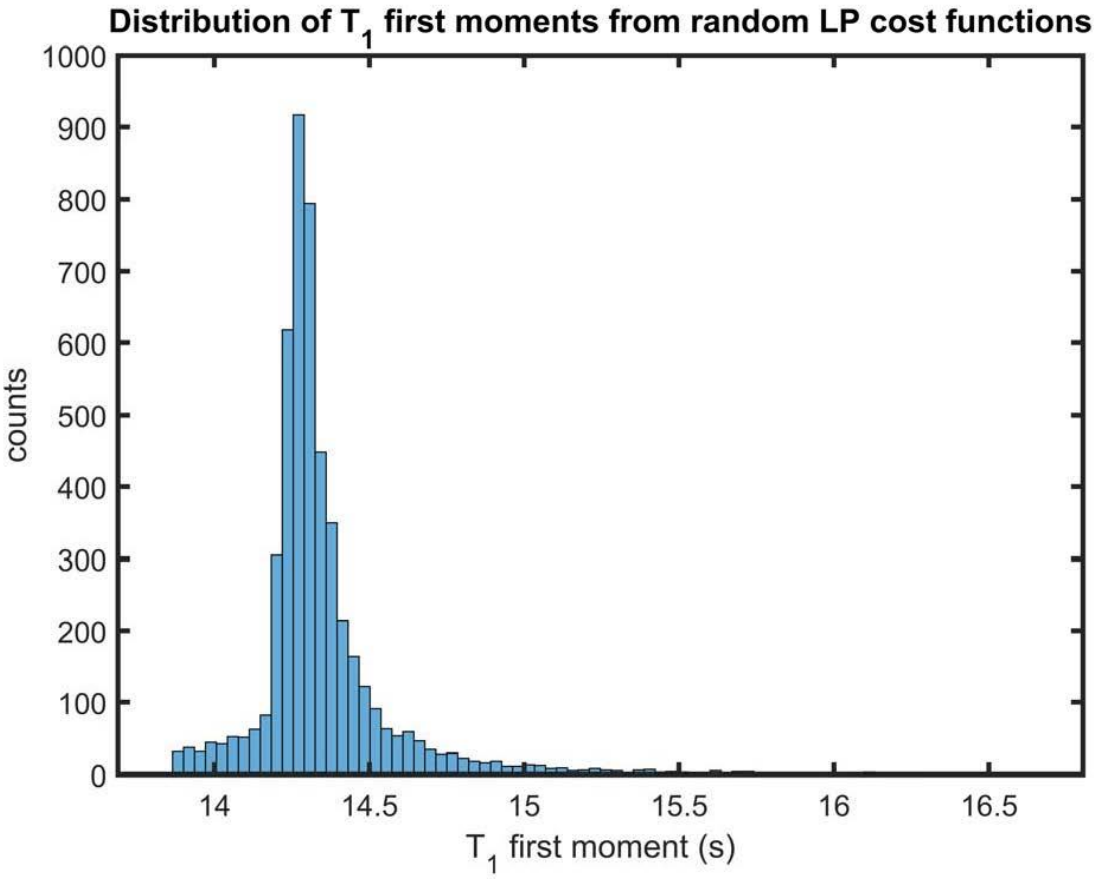

Figure 8: Histogram of the first moment for LP fits to a single spin lattice relaxation data set with 5000 random cost functions.

One of the problems with LP fits to the data is that the results do not lend themselves to estimating the error in the fits. Unlike LS, where the algorithm minimizes the difference between the fit and the data, providing a statistical means of assessing the quality of the fit, LP provides a fit, if it exists, that falls within the error tolerance set by the supplied noise value. We can sample a large number of LP fits to a given data set by varying the cost function, thereby giving us statistics on the first and second moment values that we calculate from the fits. By creating a series of cost functions, each a set of random numbers, we obtained a large number of unbiased LP fits from which we calculated the mean and standard deviation of the first and second moments. An example is shown in figure 8, where a histogram of the first moment is plotted for LP fits with 5000 random cost functions.

Conclusions

We investigated numerous materials as potential photoexcited relaxation agents. Most failed to meet one or more of the criteria for useful photoexcited relaxation agents: either they were chemically unstable or the unpaired electrons failed to produce significant nuclear relaxation. Even the one successful photoexcited relaxation agent, $[Fe(1\text{-propyltetrazole})_6](BF_4)_2$, showed only a weak photoexcited relaxation effect under the sample and experimental conditions we used. Nonetheless, there are many interesting results here that suggest future lines of investigation.

The photoexcited relaxation induced by $[Fe(1\text{-propyltetrazole})_6](BF_4)_2$ appeared small in large part because it was competing with proton relaxation induced by rotation of the methyl groups in the complex. The low concentration of methyl groups introduced with $[Fe(1\text{-propyltetrazole})_6](BF_4)_2$ reduced the spin lattice relaxation time of polystyrene by roughly a factor of 20, a very significant reduction. It suggests a potential line of investigation for future researchers: developing efficient methyl group rotation relaxation agents.

Although 1-(dibenzo[b,d]furan-2-yl)phenylmethanone (BDBF) failed to exhibit photoexcited nuclear spin relaxation, the observed lack of any line-broadening effect upon irradiation with UV result is very intriguing. The long phosphorescence lifetime and lack of NMR broadening suggest the combined Zeeman and zero-field splittings of the triplet magnetic sublevels is very large. This opens the possibility of BDBF being a photoexcited relaxation agent or a candidate for optically-excited triplet state DNP at low field. There may be limited application for relaxation rate or nuclear polarization enhancement at low field, but some NMR techniques such a field-cycling relaxometry and certain DNP experiments make use of electronically switched field or sample shuttling to rapidly move from low to high field. Such equipment could be used with BDBF to enhance relaxation or polarization at low field followed by signal detection at high field for enhanced sensitivity and resolution. This represents a potential line of investigation for future researchers.

Acknowledgments

We are very grateful for the synthetic support during the course of this program provided by two participants, Dr. Holly Ricks-Laskoski and Dr. Matthew Laskoski. They both synthesized, purified and characterized the Fe(II) and Fe(III) complexes studied here as well as the dyad molecule, which represented a challenging organic synthesis. We also are grateful to Dr. Brian Chaloux for the XPS results and Dr. Evan Glaser for the EPR results on the Fe(II) complex that suggested the presence of Fe(III) impurities.

Appendix

Three Matlab scripts for processing relaxation data as described in the Data analysis section are presented below.

Initial processing and linear programming analysis

```
%Processing_OptoRelax_data.m

%% Read the data
load FePTZ_Bruker1.mat
datdirs=who('OptoRelax_*');

%% Table template
LPTable=struct('DataSet',[],'ExpNo',[],'Sample',[],'Temperature',[],'Light',[],...
    'Data',[],'tau',[],'LP_SD',[],'LP_T1',[],'LP_weights',[],'LP_curve',[],...
    'LPexitflag',[],'phaseflag',[],'madflag',[],...
    'T1_firstmom',[],'T1_secondmom',[],'NoiseVal',[],'LPres',[]);

%% Process data
m=1;

for p=1:length(datdirs)

    eval(strcat('plotnmrdata(',datdirs{p},'.All);'));
    fid; bc; cwsub; close

    eval(strcat('L0=',datdirs{p},'.TD;'));
    eval(strcat('L1=',datdirs{p},'.TD-round(',datdirs{p},'.TD/2);'));
    eval(strcat('L2=',datdirs{p},'.TD2;'));
    eval(strcat('nsets=length(',datdirs{p},'.vdlist);'));
    eval(strcat('Lind=L2/nsets;'));

eval(strcat('Data=reshape(sum(abs(',datdirs{p},'.All.dat(2:17,:)),1),nsets,Lind);'));
    eval(strcat('SD=reshape(sqrt(16*var(abs(',datdirs{p},'.All.dat(round(end-
L1+1):end,:)),1)),nsets,Lind);'));
    eval(strcat('Tau=',datdirs{p},'.vdlist;'));
    eval(strcat('Tlims=[min(',datdirs{p},'.vdlist),', ...
        'max(',datdirs{p},'.vdlist)];'));
    nguess = 20*(ceil(log2(Tlims(2)))-floor(log2(Tlims(1))));
    T1guess = 2..^(linspace(floor(log2(Tlims(1))),ceil(log2(Tlims(2))),nguess)');
% use Median Absolute Deviation to look for outliers in the data
    madflag=median(abs(bsxfun(@minus,Data,median(Data,2))),2);
```

```
    madflag=bsxfun(@rdivide,abs(bsxfun(@minus,Data,median(Data,2))),madflag);
    madflag=madflag>3;
    madflag=sum(madflag)>3;
% add phaseflag info
    eval(strcat('phase=angle(',datdirs{p},'.FID(2,nsets:nsets:end));'));
    phaseflag=abs(phase-median(phase));
    phaseflag=phaseflag>0.2;

    Data0=zeros(L0,nsets);
    MaxData=max(max(Data));
    MaxT1=Tlims(2);

%% Fit data
    for l=1:Lind
        NoiseMin=1;
        NoiseMax=1000;
        NoiseVal=(mean([NoiseMax NoiseMin]));
        NoiseDelta=NoiseMax-NoiseMin;
        TestFlag=0;

        while NoiseDelta>.1

            LPfit=LPrelaxNMR(Tau,Data(:,l),NoiseVal*SD(:,l),[],[],T1guess,0);
            TestFlag=LPfit.flag;
            if TestFlag~=1
                NoiseMin=NoiseVal;
                NoiseVal=(mean([NoiseMax NoiseMin]));
            else
                NoiseMax=NoiseVal;
                NoiseVal=(mean([NoiseMax NoiseMin]));
            end
            NoiseDelta=NoiseMax-NoiseMin;

        end

        NoiseVal=NoiseMax;
        LPfit=LPrelaxNMR(Tau,Data(:,l),NoiseVal*SD(:,l),[],[],T1guess,0);
        LSfit=LSrelaxNMR(Tau,Data(:,l),[MaxData,MaxT1],[],[],[],0);

%% Fill table
        LPTable(m).DataSet=datdirs{p}(11:end);
        LPTable(m).ExpNo=num2str(l);
        LPTable(m).Data=Data(:,l);
        LPTable(m).tau=Tau;
        LPTable(m).Sample=BDataPars{LPTable(m).DataSet,'Sample'};
        LPTable(m).Temperature=BDataPars{LPTable(m).DataSet,'Temperature'};
        LPTable(m).Light=BDataPars{LPTable(m).DataSet,'Light'};

        LPTable(m).LP_SD=SD(:,l);
        LPTable(m).LP_T1=LPfit.T1;
        LPTable(m).LP_weights=LPfit.weights;
        LPTable(m).LP_curve=LPfit.curve;
        LPTable(m).LPexitflag=LPfit.flag;
        LPTable(m).T1_firstmom=sum(LPfit.T1.*LPfit.weights)./sum(LPfit.weights);
        LPTable(m).T1_secondmom=sum((LPfit.T1-
LPTable(m).T1_firstmom).^2..*LPfit.weights)./sum(LPfit.weights);
        LPTable(m).NoiseVal=NoiseVal;
        LPTable(m).LPres=sum(abs(LPfit.curve-Data(:,l)));

        LPTable(m).T1_LS=LSfit.pars(2);
```

```
        LPTable(m).T1_LSerr=LSfit.parserr(2);
        LPTable(m).LS_curve=LSfit.fitdat';
        LPTable(m).LSexitflag=LSfit.flag;
        LPTable(m).phaseflag=phaseflag(l);
        LPTable(m).madflag=madflag(l);
        LPTable(m).LSres=sum(abs(LSfit.fitdat'-Data(:,l)));

        m=m+1;
    end

end

%% Finalize table
LPTable=struct2table(LPTable);

clear Data Data0 l L0 L1 L2 Lind LPfit LSfit m MaxData MaxData0 MaxT1 nguess
NoiseDelta NoiseMax NoiseMin NoiseVal nsets p SD SD0 T1guess Tau TestFlag Tlims
```

Additional linear programming analysis for statistics

```
%FePTZ_table_update.m

load('FePTZ_Bruker1_Tablen1.mat')

biexp = zeros(410,1);
Noisef = zeros(410,1);
Wmax = zeros(410,1);
M0stat = zeros(410,2);
M1stat = zeros(410,2);
M2stat = zeros(410,2);
Nnoise = 500;
WVAR = 1.0;

for k=1:410
    Noisef(k) =
2*max(cell2mat(LPTablen{k,'LP_SD'}))*LPTablen{k,'NoiseVal'}/sum(cell2mat(LPTablen{k,'L
P_weights'}));
    biexp(k) = sqrt(LPTablen{k,'T1_secondmom'})/LPTablen{k,'T1_firstmom'};
    Wmax(k) =
max(cell2mat(LPTablen{k,'LP_weights'}))/sum(cell2mat(LPTablen{k,'LP_weights'}));

    M0 = zeros(Nnoise,1);
    M1 = zeros(Nnoise,1);
    M2 = zeros(Nnoise,1);
%     fitdata = zeros(length(cell2mat(LPTablen{k,'tau'})),Nnoise);
    decays = 1-exp(-cell2mat(LPTablen{k,'tau'})*cell2mat(LPTablen{k,'LP_T1'})'.^-1);
    Rdata = cell2mat(LPTablen{k,'Data'});
    Rnoise = 2*cell2mat(LPTablen{k,'LP_SD'})*LPTablen{k,'NoiseVal'};
    A = [decays; -decays];
    b = [Rdata+Rnoise; -Rdata+Rnoise];
    ub = [];
    lb = zeros(size(cell2mat(LPTablen{k,'LP_T1'})))';
    opts.MaxIter = 5e3;
    opts.Display = 'off';
    warning('off','all')
```

```
    if LPTablen{k,'LPexitflag'} ~= 1
        M0stat(k,:) = [0 0];
        M1stat(k,:) = [0 0];
        M2stat(k,:) = [0 0];
    else
        m = 1; n = 1;
        rng('default')
        w = ones(size(cell2mat(LPTablen{k,'LP_T1'})))';
        while m <= Nnoise
            fprintf('%d', k); fprintf('%c', ' '); fprintf('%d', n);
            pause(.005);
            [weights, ~, flag] = linprog(w,A,b,[],[],lb,ub,[],opts);
            w = 1-WVAR*rand(size(cell2mat(LPTablen{k,'LP_T1'})))';
            if flag == 1
                M0(m) = sum(weights);
                M1(m) = sum(weights.*cell2mat(LPTablen{k,'LP_T1'}))./M0(m);
                M2(m) = sum(weights.*cell2mat(LPTablen{k,'LP_T1'}).^2)./M0(m);
    %             fitdata(:,m) = sum(bsxfun(@times,decays,weights(m,:)),2);
                m = m+1;
            end
            for l=1:floor(log10(k))+floor(log10(n))+3
                fprintf('\b')
            end
            n = n+1;
        end
        M0stat(k,:) = [mean(M0) std(M0)];
        M1stat(k,:) = [mean(M1) std(M1)];
        M2stat(k,:) = [mean(M2) std(M2)];
    end
end

fprintf('\n')

LPTablen_ext = LPTablen;
LPTablen_ext.Biexp = biexp;
LPTablen_ext.Noisef = Noisef;
LPTablen_ext.Wmax = Wmax;
LPTablen_ext.M0stat = M0stat;
LPTablen_ext.M1stat = M1stat;
LPTablen_ext.M2stat = M2stat;
```

Combine results

```
% TstatsT1s.m

% load('FePTZ_Bruker1_Tablen1_extp10.mat')

DataSet=[]; Sample=[]; Temperature=[]; Light=[]; NoSets=[]; T1mean=[]; M1statavg=[];

for k=505:638
    PData=LPTablen_ext(ismember(LPTablen_ext.DataSet,{num2str(k)}) & ...
```

```
        LPTablen_ext.NoiseVal<12 & ...
        ~(LPTablen_ext.phaseflag | LPTablen_ext.madflag) & ...
        LPTablen_ext.LPexitflag==1,{'DataSet', 'Sample', 'Temperature', 'Light',
'T1_firstmom', 'M1stat'});
    PData=PData(abs(PData{:,'T1_firstmom'}-median(PData{:,'T1_firstmom'}))...
        ./median(abs(PData{:,'T1_firstmom'}-median(PData{:,'T1_firstmom'})))<=2,:);
    if ~isempty(PData)
        tabsize=size(PData,1);
        M1dat=PData{:,'M1stat'};
        M1mean=M1dat(1,1);
        M1std=M1dat(1,2);
        Na=500;
        Nb=Na;
        navg=1;
        for m=2:tabsize
            NN=Na+Nb;
            M1std=sqrt((Na*(Na-1)/(NN*(NN-1))*M1dat(m,2)/Na+...
                       Nb*(Nb-1)/(NN*(NN-1))*M1std/Nb+...
                       Na*Nb*(M1mean-M1dat(m,1))^2/NN/(NN*(NN-1))*NN));
            M1mean=(M1mean*navg+M1dat(m,1))/(navg+1);
            Nb=Nb+Na;
            navg=navg+1;
        end
        DataSet=[DataSet; PData{1,'DataSet'}];
        Sample=[Sample; PData{1,'Sample'}];
        Temperature=[Temperature; PData{1,'Temperature'}];
        Light=[Light; PData{1,'Light'}];
        NoSets=[NoSets; tabsize];
        T1mean=[T1mean; mean(PData{:,'T1_firstmom'})];
        M1statavg=[M1statavg; [M1mean M1std]];
    end
end


LPTablen_avg=table(DataSet, Sample, Temperature, Light, NoSets, T1mean, M1statavg);
```

References

[1] R. G. Walker and W. Happer, *Rev. Mod. Phys.*, **69**, 629 (1997).
[2] S. J. Opella, *Nature Methods*, **6**, 197 (2009).
[3] G. Pintacuda and G. Kervern, *Top. Curr. Chem.*, **335**, 157 (2013).
[4] C. P. Jaroniec, *J. Magn. Reson.*, **253**, 50 (2015).
[5] M. Bertmer, *Sol. St. Nucl. Magn. Reson.*, **81**, 1 (2017).
[6] T. Maly, G. T. Debelouchina, V. S. Bajaj, K. Hu, C. Joo, M. L. Mak-Jurkauskas, J. R. Sirigiri, P. C. van der Wel, J. Herzfeld, R. J. Temkin, and R. G. Griffin, *J. Chem. Phys.*, **128**, 052211 (2008).
[7] P. Beckmann, S. Clough, J. W. Hennel, and J. R. Hill, *J. Phys. C: Solid State Phys.*, **10**, 729 (1977).
[8] M. G. Zysmilich and A. McDermott, *J. Am. Chem. Soc.*, **116**, 8362 (1994).
[9] R. Eisenberg, *Acc. Chem. Res.*, **24**, 110 (1991).
[10] R. Tycko, *Solid State Nucl. Magn. Reson.*, **11**, 1 (1998).
[11] A. Ajoy, R. Nazaryan, E. Druga, K. Liu, A. Aguilar, B. Han, M. Gierth, J.T. Oon, B. Safvati, R. Tsang, J.H. Walton, D. Suter, C.A. Meriles, J.A. Reimer, and A. Pines, *Rev. Sci. Instrum.*, 91, 13 (2020).
[12] A. Hauser, *Top. Curr. Chem.*, **234**, 155 (2004).
[13] M. F. Tweedle and L. J. Wilson, *J. Am. Chem. Soc*., **98**, 4824 (1976).
[14] X.W. Feng, C. Mathoniere, I.R. Jeon, M. Rouzieres, A. Ozarowski, M.L. Aubrey, M.I. Gonzalez, R. Clerac, and J.R. Long, *J. Am. Chem. Soc.*, **135**, 15880 (2013).
[15] J. P. Yesinowski , J. B. Miller, C. A. Klug, and H. L. Ricks-Laskoski, *Sol. St. Nucl. Magn. Reson.*, **96**, 1 (2018).
[16] M. M. Dırtu, C. Neuhausen, A. D. Naik, A. Rotaru, L. Spinu, and Y. Garcia, *Inorg. Chem.*, **49**, 5723 (2010).
[17] T. Mani, D. M. Niedzwiedzki, and S. A. Vinogradov, *J. Phys. Chem. A*, **116**, 3598 (2012).
[18] M. G. Zysmilich and A. McDermott, *J. Am. Chem. Soc*., **118**, 5867 (1996).
[19] C. E. D. Chidsey, L. Takiff, R. A. Goldstein, and S. G. Boxer, *Proc. Natl. Acad. Sci. USA*, **82**, 6850 (1985).
[20] E. Busby, , J. Xia, , Qin Wu, , J. Z. Low, , R. Song, , J. R. Miller, , X-Y. Zhu, L. M. Campos, and M. Y. Sfeir, *Nature Materials*, **14**, 426 (2015).
[21] E. Kumarasamy, S. N. Sanders, M. J. Y. Tayebjee, A. Asadpoordarvish, T. J. H. Hele, E. G. Fuemmeler, A. B. Pun, L. M. Yablon, J. Z. Low, D. W. Paley, J. C. Dean, B. Choi, G. D. Scholes, M. L. Steigerwald, N. Ananth, D. R. McCamey, M. Y. Sfeir, and L. M. Campos, *J. Am. Chem. Soc.*, **139**, 12488 (2017).
[22] K. R. Parenti, G. He, S. N. Sanders, A. B. Pun, E. Kumarasamy, M. Y. Sfeir, and L. M. Campos, *J. Phys. Chem. A*, **124**, 9392 (2020).
[23] W. Zhao, Z. He, J. W.Y. Lam, Q. Peng, H. Ma, Z. Shuai, G. Bai, J. Hao, and B. Z. Tang, *Chem*, **1**, 592 (2016).
[24] K. Tateishi, M. Negoro, S. Nishida, A. Kagawa, Y. Morita, and M. Kitagawa, *PNAS*, **111**, 7527 (2014).
[25] C. Leys, C. Ley, O. Klein P. Bernard, L., and Licata, *J. Exp. Social Psych.*, **49**, 764 (2013).
[26] K. P. Whittall and A. L. MacKay, *J. Magn. Reson.*, **84**, 134 (1989).